Available online at www.sciencedirect.com
SCIENCE DIRECT®
Journal of Nuclear Materials 354 (2006) 85–93
journal of nuclear materials
www.elsevier.com/locate/jnucmat

Oxidation behaviour of unirradiated sintered UO_2 pellets and powder at different oxygen partial pressures, above 350 °C

F. Valdivieso [a,*], V. Francon [a], F. Byasson [a], M. Pijolat [a], A. Feugier [b], V. Peres [b]

[a] *Laboratoire des Procédés en Milieux Granulaires CNRS UMR 5148, Centre SPIN, Ecole Nationale Supérieure des Mines, 158 Cours Fauriel, 42023 Saint-Etienne cedex 2, France*
[b] *FBFC – FRAMATOME – ANP, Les Bérauds, BP 1114, 26104 Romans cedex, France*

Received 21 February 2005; accepted 15 February 2006

Abstract

The oxidation of sintered UO_2 pellets and powder into U_3O_8 has been studied by thermogravimetry at 370 °C, under controlled oxygen partial pressures (P_{O_2} ranging from 2 to 40 kPa). Sigmoidal curves of oxidation weight gain were measured for both pellet and powder test samples. The rate of oxidation increased as the oxygen partial pressure increased. It has been shown, by simultaneous TG-DSC, that the reaction proceeds in a pseudo steady state. An experimental methodology based on temperature or P_{O_2} jumps has shown that the assumption of a rate-limiting step is validated, and a mean value of activation energy for the formation of U_3O_8 of 103 kJ mol^{-1} was estimated.

1. Introduction

The oxidation of UO_2 into U_3O_8 has been studied extensively for several years [1–3], because it is an important process in performance analysis for the dry storage and ultimate disposal of spent nuclear fuel. The formation of U_3O_8 by oxidation of UO_2 corresponds to 36% increase in volume. This volume increase leads to further degradation of a defective fuel cladding and to the release of radioactive U_3O_8 powder in the storage container. Also, the formation of U_3O_8 increases significantly the surface area of the spent fuel from that of UO_2 pellet fragments. Consequently, detailed knowledge of the kinetics of the formation of U_3O_8 is needed in order to define safe conditions of storage. For this reason, most studies previously reported focused on oxidation behaviour at rather low temperatures (200–300 °C) [1,4–13]. The purpose and background of our work is quite different. It consists of investigating the oxidation of sintered UO_2 pellets and powder at higher temperatures above 350 °C. Information from these investigations will be used to optimise the calcination in air of recycled UO_2, which is one of the industrial process steps to manufacture nuclear fuel.

It has been shown [1] that the oxidation of UO_2 is at least a two-step reaction, usually written as $UO_2 \rightarrow U_4O_9/U_3O_7 \rightarrow U_3O_8$.

* Corresponding author. Tel.: +33 4 7742 0291; fax: +33 4 7749 9694.
E-mail address: fvaldivieso@emse.fr (F. Valdivieso).

0022-3115/$ - see front matter © 2006 Elsevier B.V. All rights reserved.
doi:10.1016/j.jnucmat.2006.02.096

With powders, the intermediate phases U_4O_9 and U_3O_7 are more or less clearly observed up to about 200–250 °C [4,5,9–11]; above 250 °C, U_3O_8 appears [1,5,11]. The reaction curves exhibit a first step with a continuously decreasing rate, corresponding to the U_4O_9/U_3O_7 formation, then during the oxidation into U_3O_8 they display a sigmoidal shape, often attributed to nucleation and growth behaviour and more generally to reaction area changes. Above 350 °C, the intermediate phases U_4O_9/U_3O_7 are generally not observed, the oxidation seems to proceed directly to U_3O_8 [5,11].

The temperatures leading to a significant oxidation of sintered UO_2 pellets are higher (about 300–350 °C) and it seems that if only a thin layer of U_3O_7 is formed on the surface of the pellets [12,13], then the oxidation to U_3O_8 proceeds according to only sigmoidal reaction curves. At higher temperatures (above 350 °C), only U_3O_8 is observed [14].

Concerning the effect of oxygen pressure, there is no universal agreement in the case of U_4O_9/U_3O_7 formation on powders [2,9,10]. The parabolic rate constant corresponding to the formation of U_3O_7 has been measured at temperatures ranging from 130 to 200 °C, and oxygen partial pressures varying between 0.003 and 101 kPa. A slight oxidation increasing effect is observed when $P_{O_2} < 20$ kPa [9,10], whereas it seems that there is no significant effect if $P_{O_2} > 20$ kPa [9]. For sintered UO_2 pellets, the influence of the oxygen partial pressure has been considered separately for the 'induction' and 'post-induction' (rapid and 'linear' oxidation) periods of the sigmoidal curves. The literature [2] reports no effect on the induction period rates, but show that the oxidation rate in the 'linear' part of the sigmoidal curves increases as P_{O_2} increases.

The sigmoidal curves are usually interpreted using the Avrami [15] or Johnson–Mehl [16] models. But these models assume that the nucleation occurs throughout the volume of the existing phase, rather than only at the surface of the grains. Thus, from a physico-chemical point of view, they are not appropriated to the oxidation of sintered UO_2 pellets or powders (even though these models can be used to 'approximate' closely the shape of the reaction curves).

Finally, despite the numerous studies dedicated to the formation of U_3O_8, this reaction is not yet fully understood. In particular, there is a wide range of reported values for the activation energy of U_3O_8 formation [17]. These values depend on the method of data analysis used by the authors to estimate an activation energy; such as from the 'linear part of the sigmoidal curves', from the 'maximum rate', from the time necessary for '50% conversion to U_3O_8', etc. Thus, the literature data on the oxidation of UO_2 at temperatures higher than 350 °C is ambiguous. For this reason, we studied the oxidation of industrial sintered UO_2 pellets and powder, at controlled oxygen partial pressure and temperature at 370 °C. This is an approach we have used in previous oxidation studies [18–20]. With this approach, the validity of existing kinetic assumptions discussed in the literature can be experimentally determined. In particular:

(i) the pseudo steady state assumption (which is necessary to assume the existence of a rate-limiting step) can be verified by measuring the reaction rate with two techniques (for example, simultaneous thermogravimetry and calorimetry [18–20]): if the system proceeds in a pseudo steady state, the rates of weight gain and the heat flow should remain proportional during the whole reaction,

(ii) the assumption of a rate-limiting step can be verified using a method based on temperature or pressure jumps [18–20]. When phase transformations in solids are modelled, the rate is usually written as

$$\frac{d\alpha}{dt} = A \exp\left(-\frac{E_a}{RT}\right) f(\alpha), \quad (1)$$

where α is the fractional conversion, A is called the pre-exponential factor, E_a is the activation energy and $f(\alpha)$ is an analytical function (which describes the evolution with time of the reaction area where the rate-limiting step of the phase transformation is located, it depends on the shape of the grains and the step controlling the growth [21,22]).

Eq. (1) implies that the rate is controlled by a step following the Arrhenius law (which is not always the case, for example when an adsorption step is involved, following Langmuir isotherm). Eq. (1) also implies that the rate is fixed by the value of α ($f(\alpha)$), which may not be the case, particularly when nucleation and growth processes are in competition [23].

We propose a more general expression for the fractional conversion rate function, given in the following expression:

$$\frac{d\alpha}{dt} = \Phi(T, P_i)E(t) \quad (2)$$

in which Φ is a rate per unit area (mol m^{-2} s^{-1}), depends on the nature of the rate-limiting step (diffusion, interface reaction), may be a function of temperature T and of the partial pressures of the reacting gases P_i, but is independent of time. $E(t)$ (in m^2 mol^{-1}) corresponds to the extent of the reaction zone where the rate-limiting step is spatially located. The interest of the general expression Eq. (2) is that it only assumes the existence of a rate-limiting step for the oxidation of UO_2 to U_3O_8, but no additional explicit assumption is made concerning the nature and the localisation of this step (however, it is expressed in the $E(t)$ function).

Once points (i) and (ii) have been validated experimentally, Eq. (2) can be used. Then the jump method, in which variations of T and P_i are made, is used to experimentally evaluate the variations in the function $\Phi(T, P_i)$. This testing method is very useful for identifying the rate-limiting step and verifying a conversion mechanism. It also makes it possible to determine experimentally whether the conversion rate is consistent with any of the possible $f(\alpha)$ function choices available in the literature [23].

Thus, in this article we have tried to answer these questions, for the problem of oxidation of UO_2 into U_3O_8 at high temperature:

- Does the oxidation of UO_2 into U_3O_8 proceed in a pseudo steady state?
- Is there a rate-limiting step?
- If a rate-limiting step does exist, what is the influence of the oxygen partial pressure on the oxidation rate?
- Can we determine an activation energy for the formation of U_3O_8?

2. Experimental

The test specimens were UO_2 pellets and UO_2 powder with large agglomerates, supplied by the industry Franco-Belge de Fabrication du Combustible (FBFC-FRAMATOME-ANP). The pellets were 8.2 mm in diameter and 1.9 mm in height. The mean UO_2 grain size is about 10 μm, as shown on the micrograph in Fig. 1. The agglomerated powder was prepared from the starting powder, by calcination at 1700 °C under hydrogen during 4 h (using the pellet sintering cycle). Its specific surface area, measured by nitrogen adsorption at 77 K (BET method), is 0.031 m^2 g^{-1}. It is constituted by agglomerates of about 100 μm (Fig. 2(a)), in which the grain size varies between 2 and 10 μm approximately (Fig. 2(b)).

The oxidation curves were obtained under isothermal and isobaric conditions with a symmetrical

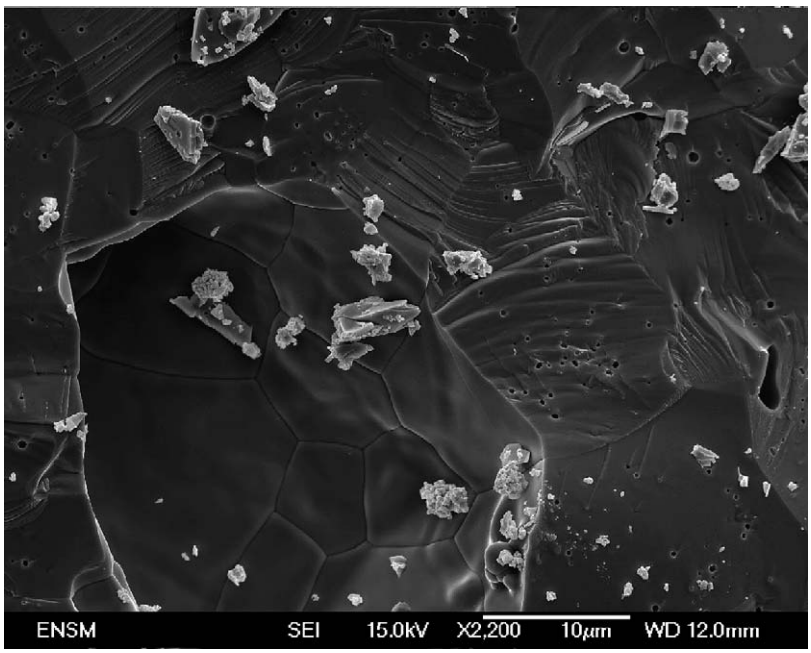

Fig. 1. Micrograph of a fragment of a sintered UO_2 pellet.

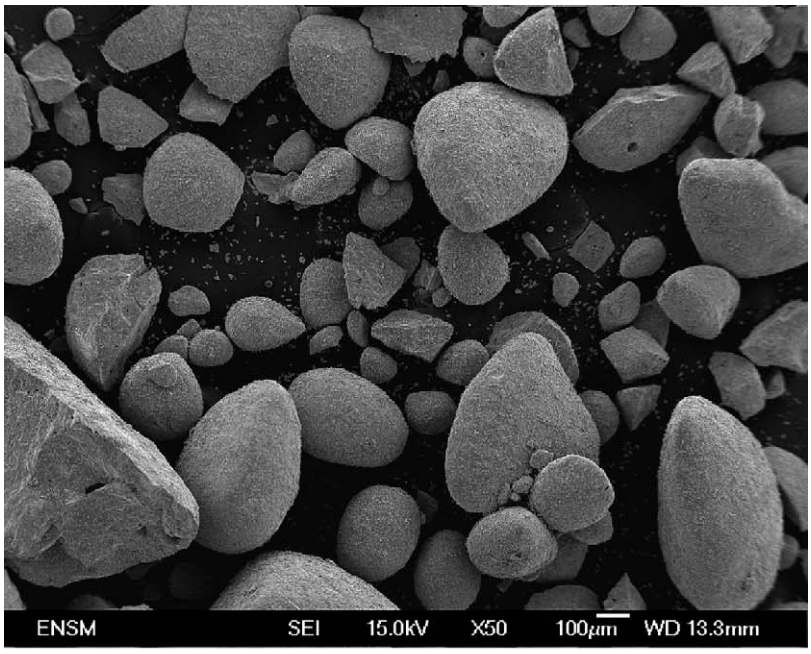

a

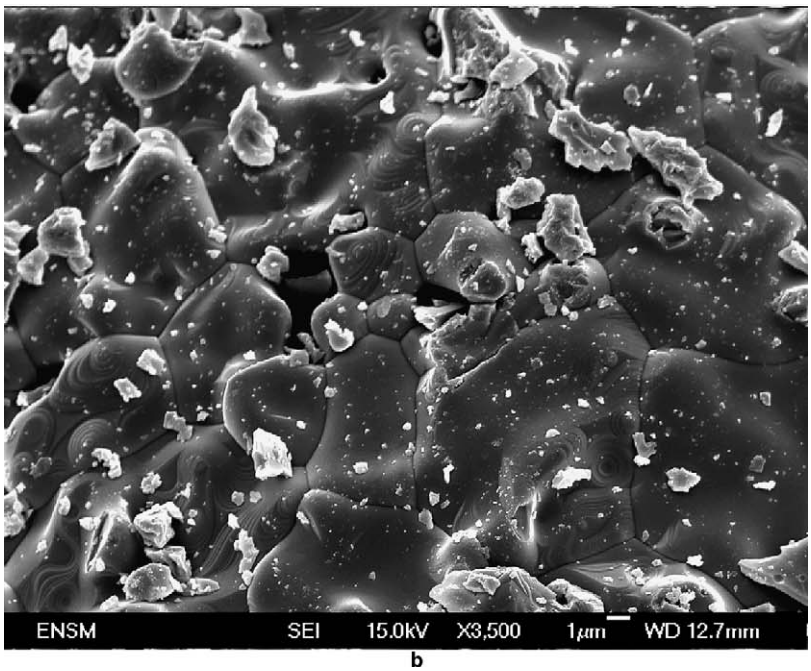

b

Fig. 2. Micrograph of the UO_2 powder (a) and magnification of one of the agglomerates (b).

thermoanalyser SETARAM TG-DSC 111, under a flowing mixture of oxygen in helium. The flowrates of the gases are controlled by mass-flowmeters (Brooks 5850S), the total flowrate being $2\,l\,h^{-1}$. The partial oxygen pressure could be controlled within the range of 2–40 kPa. The jump method tests with oxygen pressure changes were performed by changing quickly the calibrated oxygen flowmeter setpoint. The thermoanalyser software allows to control and record the temperature of the furnace. The signals corresponding to the weight gain and the heat flow are also recorded continuously.

Some experiments have been carried out in a symmetrical thermobalance under static atmosphere (SETARAM MTB 10^{-8}, the total pressure being the oxygen pressure fixed for the experiment). In that case, the temperature of the sample and the weight gain are recorded continuously.

In order to identify the phases formed during the oxidation of UO_2 pellets and powder, XRD experiments were carried out on a Siemens D5000 diffractometer (Cu K_α radiation, step: 0.015°, step time: 5 s).

3. Results

3.1. Shape of the oxidation curves, effect of temperature

Fig. 3 shows kinetic curves giving the fractional conversion α of sintered UO_2 pellets versus time, at three different temperatures (260, 370, 500 °C), and a partial oxygen pressure of 20 kPa. The fractional conversion is calculated from the weight gain ($\Delta m(t)$), using the following equation:

$$\alpha = \frac{\Delta m(t)}{\Delta m(\text{theo})}, \tag{3}$$

where Δm(theo) is the theoretical weight gain corresponding to the total oxidation into U_3O_8 (3.95%).

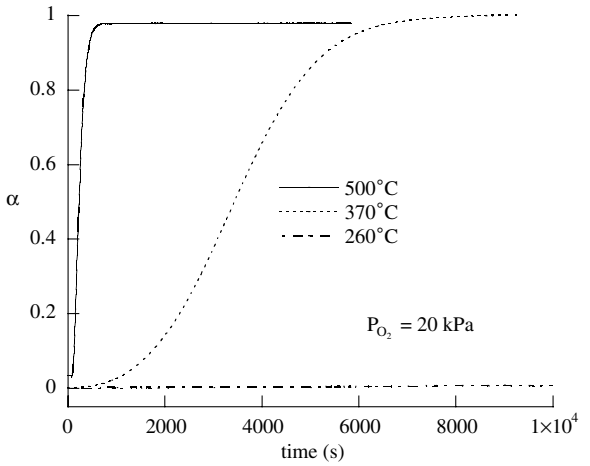

Fig. 3. Fractional conversion versus time for sintered UO_2 pellets at an oxygen partial pressure of 20 kPa, at 260, 370 and 500 °C.

No significant oxidation occurs at 260 °C during the time investigated, a sigmoidal curve is observed at 370 °C and the oxidation is very rapid at 500 °C. In the results that follow, the experiments were mostly performed at 370 °C, and a few experiments were at 600 °C. The U_3O_8 formed on the sintered UO_2 pellets spalls from the surface as a powder. Its specific surface area (measured by nitrogen adsorption at 77 K according to the BET method)

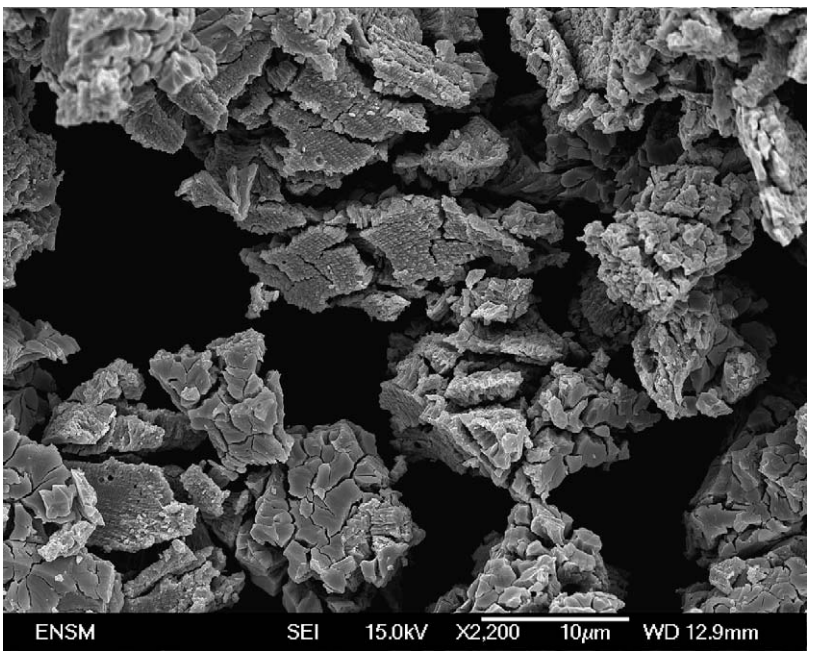

Fig. 4. Micrograph of the U_3O_8 powder obtained by oxidation of a UO_2 pellet (370 °C, $P_{O_2} = 20$ kPa).

decreases when the oxidation temperature increases: it is equal to 0.8 $m^2 g^{-1}$ at 370 °C, and 0.5 $m^2 g^{-1}$ at 600 °C. The U_3O_8 spallation particles have approximately the same size as the original UO_2 grains, but have highly fractured microcracked features that are shown on the micrograph in Fig. 4. The possible oxide phases present in oxidized samples were studied by X-ray diffraction. Prior to oxidation, only the UO_2 phase was observed on sintered pellets and powder. A pellet partially oxidized up to a weight gain of 1.9% (theoretical weight gain corresponding to the oxidation into U_3O_7) exhibits the diffraction peaks of UO_2 and U_3O_8: no U_3O_7 is detected in this sample, or in a sample oxidized to a lower weight gain (1%). However, the quantity of U_3O_7 that forms may be too small to be detected by XRD. In the following kinetic analysis, we will assume that the UO_2 phase is transformed directly into a U_3O_8 phase without any intermediate phases.

3.2. Effect of oxygen pressure

Fig. 5 shows $\alpha(t)$ kinetic curves obtained at 370 °C with sintered UO_2 pellets (Fig. 5(a)) and powder (Fig. 5(b)): here, it is seen that the higher the oxygen partial pressure, then the higher the oxidation rate. However, the oxygen partial pressure influence is greater for lower pressures ($P_{O_2} \leqslant 10$ kPa), and the oxygen partial pressure effect decreases between 10 and 20 kPa. In Fig. 6, it is seen that under the same conditions (370 °C, $P_{O_2} = 20$ kPa), the powder is fully oxidised more rapidly than a sintered pellet. This is a clear indication of the surface area dependence on the oxidation conversion rates of UO_2 to U_3O_8.

3.3. Pseudo steady state assumption

Fig. 7(a) shows both the rate of weight gain (dm/dt) and the heat flow (dQ/dt) versus time at 370 °C and 20 kPa of oxygen partial pressure, for a sintered pellet. The curves are superimposed during the whole reaction, which indicates that the reaction system is in a pseudo steady state. The data curves can be superimposed for experiments performed at different oxygen partial pressures, and with powdered samples. The constant ratio between the rate of weight gain and the heat flow is given by

$$\frac{dQ}{dt} = \frac{\Delta H}{1/3 M_{O_2}} \frac{dm}{dt}, \quad (4)$$

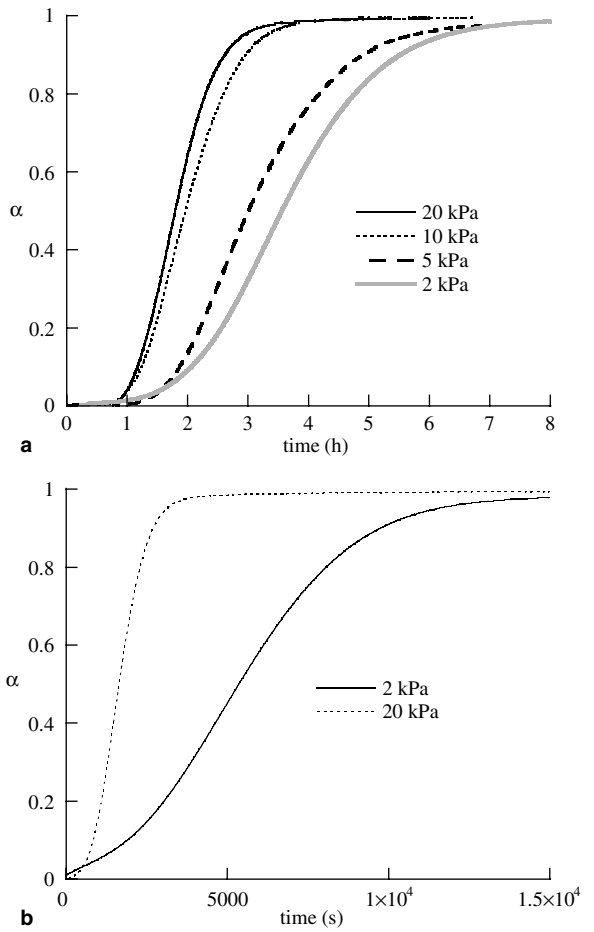

Fig. 5. Fractional conversion α versus time for various oxygen pressures at 370 °C, for UO_2 pellets (a) and powder (b).

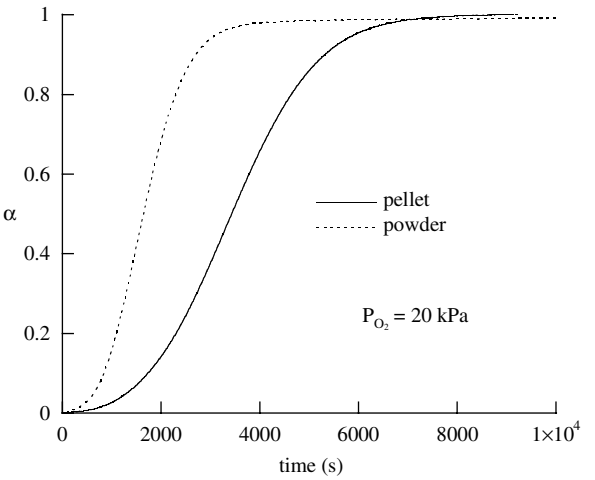

Fig. 6. Fractional conversion α versus time for a powder and a sintered pellet in the same conditions of oxidation ($T = 370$ °C, $P_{O_2} = 20$ kPa).

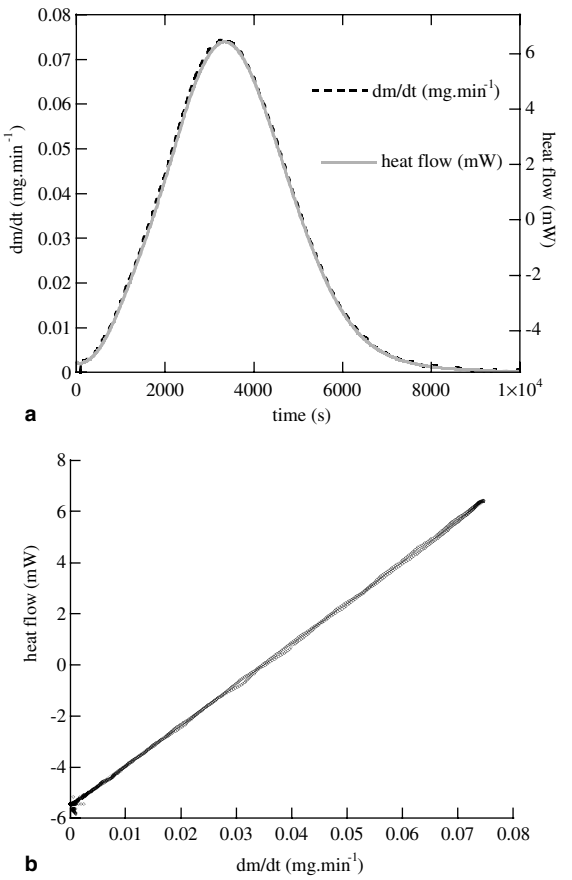

Fig. 7. Rate of weight gain (--- dm/dt) and heat flow (— dQ/dt) versus time for a sintered UO_2 pellet at 370 °C in oxygen (20 kPa) (a), and dQ/dt versus dm/dt (b) to verify the linear relationship (Eq. (4)).

where M_{O_2} is the molar mass of oxygen, and ΔH the enthalpy of the reaction (E1):

$$UO_2 + 1/3O_2 = 1/3U_3O_8 \quad \text{(E1)}$$

Using the linear relationship (Eq. (4)) between $\frac{dQ}{dt}$ and $\frac{dm}{dt}$, represented in Fig. 7(b), it is possible to estimate the value of the enthalpy of the reaction (E1) for several isothermal and isobaric experiments. The result $\Delta H = 101 \pm 2$ kJ mol^{-1}, is in close agreement with the value calculated using thermodynamic tables [24]: $\Delta H_{calc} = 103$ kJ mol^{-1} at 370 °C.

3.4. Rate-limiting step assumption

If a single rate-limiting step exists, Eq. (2) can be applied to describe the variations of the oxidation conversion rate with the intensive variables (T, P_i...) and time, t. In isobaric and isothermal conditions, the variations of the rate with time are given by $E(t)$, and $\Phi(T, P_i)$ remains constant. A sudden change (jump) in temperature or partial pressure during an experiment will then lead to a change in Φ only, while $E(t)$ will remain approximately constant during the jump time interval (provided that the time interval necessary for the T or P_i change is short enough: in this case, it takes about 5 min, the whole experiment lasting 120–180 min (2–3 h)). Thus the ratio of the rates measured after (to the right) and before (to the left) of the jump is equal to $\frac{\Phi_r}{\Phi_l}$ ($E(t)$ dependence is eliminated in the ratio). Performing a series of similar jump experiments at different reaction times, or equivalently values of α, provides a set of $\frac{\Phi_r}{\Phi_l}$ ratios, one for each time. And if each of ratios $\frac{\Phi_r}{\Phi_l}$ obtained from the series of experiments is equal, then Eq. (2) is an acceptable model expression. This method, which we have named the '$\Phi \cdot E$ test', has been successfully used in several previous experiments [18–20]. The results obtained with sintered pellets are indicated in Fig. 8. The sudden changes in temperature ranged from 360 to 390 °C ($P_{O_2} = 20$ kPa, Fig. 8(a)) and the sudden changes in oxygen pressure ranged from 2 to 20 kPa ($T = 370$ °C, Fig. 8(b)). Considering the experimental error bars, the ratio of the rates measured on both sides of the jumps remained approximately at a constant value, independent of the fractional conversion α. Consequently, it is concluded that the conversion rate model of Eq. (2) is validated. As the pseudo steady state assumption is also verified, the assumption of a single rate-limiting step for the U_3O_8 growth mechanism is valid. This implies that the oxidation of UO_2 to U_3O_8, at high temperatures (about 350 °C), can be analysed with a model given by Eq. (2).

3.5. Variations of Φ with respect to partial oxygen pressure changes

The variations of Φ with respect to a partial gas pressure P_i can easily be obtained by performing sudden changes, from P_0 to P_i, at a given fractional conversion α. At constant temperature and using Eq. (2), the ratio of the rates are equal to $\frac{\Phi(P_i)}{\Phi(P_0)}$ [18–20,25]. A series of experiments were carried out on sintered pellets at 370 °C, with oxygen partial pressures varying from 2 kPa (P_0) to 40 kPa after the jump. The variations of Φ with P_{O_2} are shown in Fig. 9, for pressure jump experiments at two fractional conversions ($\alpha = 0.2$ and $\alpha = 0.5$). The data error bars overlap, which is in agreement with Eq.

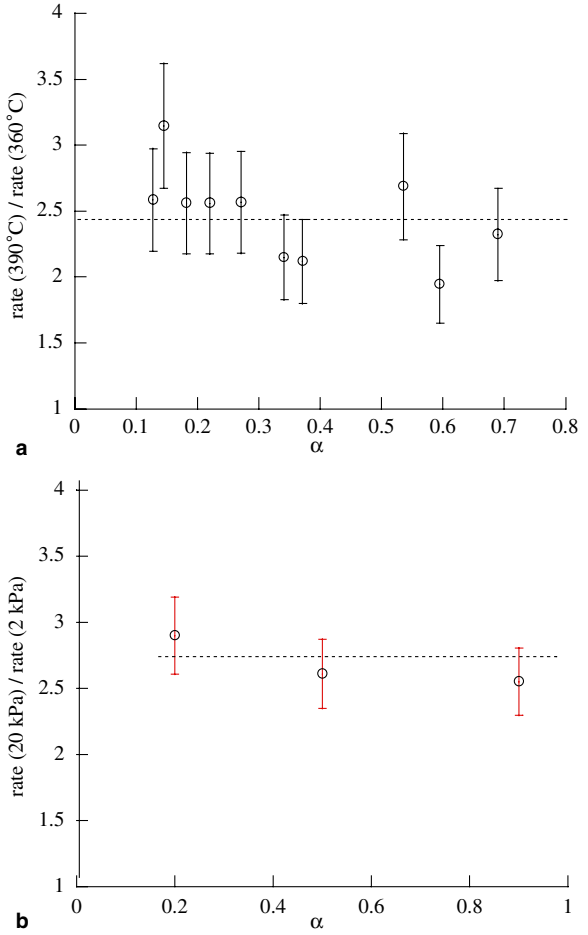

Fig. 8. Ratios of the rate of weight gain before and after temperature jumps ($P_{O_2} = 20$ kPa) (a) and oxygen pressure jumps ($T = 370$ °C) (b).

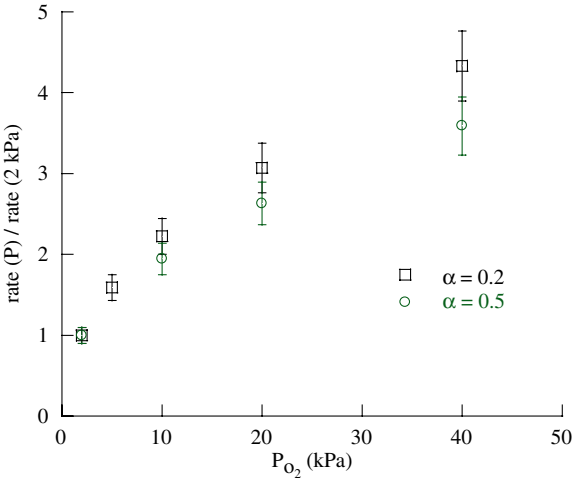

Fig. 9. Variation of Φ with the partial oxygen pressure for a sintered pellet (jumps from $P_{O_2} = 2$ kPa to P, for $\alpha = 0.2$ and 0.5, $T = 370$ °C).

(2), and the increasing oxygen partial pressure experimental data show an increasing $\Phi(P_{O_2})$ function for U_3O_8 conversion.

3.6. Estimation of the activation energy for the formation of U_3O_8

Using the temperature jumps (from 360 to 390 °C) made for the '$\Phi \cdot E$' test data, it is possible to estimate an apparent Arrhenius activation energy for the formation of U_3O_8. Writing the Φ function as

$$\Phi(T, P_{O_2}) = A_0 \exp\left(-\frac{E_a}{RT}\right) f(P_{O_2}), \tag{5}$$

the ratio of the rates on both sides for only the temperature jump experiments is then

$$\frac{\Phi(T_1, P_{O_2})}{\Phi(T_0, P_{O_2})} = \exp\left(-\frac{E_a}{R}\left(\frac{1}{T_1} - \frac{1}{T_0}\right)\right), \tag{6}$$

and thus

$$E_a = \frac{RT_0T_1}{T_1 - T_0} \ln\left(\frac{\Phi(T_1, P_{O_2})}{\Phi(T_0, P_{O_2})}\right). \tag{7}$$

The values of E_a calculated from the temperature jump data made at different fractional conversions α (see Fig. 8(a)) are provided in Table 1. The activation energy estimated values are in the range 77–133 ± 15 kJ mol^{-1}, and they depend somewhat on the value of α. The mean value is 103 kJ mol^{-1}, which is situated within an order of magnitude of the activation energy values reported in the literature data for pellets above 300 °C [17]. It is worth noticing that the activation energy estimated in this work is obtained directly from experiments without

Table 1
Values of the activation energy E_a of the formation of U_3O_8, obtained from temperature jump experiments (360–390 °C) at different fractional conversions α

Fractional conversion α	0.12	0.15	0.18	0.22	0.27	0.34	0.37	0.53	0.6	0.7
E_a (kJ mol^{-1}) ± 15 kJ mol^{-1}	110	133	109	109	109	89	87	115	77	98

any explicit analysis of the $\alpha(t)$ curves; and the only assumption is that the Arrhenius law applies.

Conversely, if Arrhenius temperature kinetics are followed, then all data from the temperature jump experiments should provide the same estimated value for activation energy E_a, independently of the fractional conversion α. This is approximately the case (considering the error bars on the temperature jumps).

4. Conclusions

The oxidation of sintered UO_2 pellets and powder to U_3O_8 has been studied at 370 °C under a controlled partial oxygen pressure, P_{O_2}. Sigmoidal curves have been obtained in both cases, and an increasing effect due to P_{O_2} was observed. It has been shown that the reaction proceeds in a pseudo steady state, and the assumption of a rate-limiting step has been validated using the jump method. Using temperature jump experiments, it has been verified that the oxidation rate for the formation of U_3O_8 at high temperature (~350 °C) follows the Arrhenius law. A mean activation energy was estimated for the formation of U_3O_8 of about 103 kJ mol^{-1} at 370 °C.

Further work is necessary to propose a mechanism involving elementary stages (oxygen adsorption, interface steps, diffusions) and U_3O_8 point defects, in order to describe the conversion of UO_2 to U_3O_8. Using the assumption of a rate-determining step, it would be possible to calculate theoretical laws for $\Phi(P_{O_2})$. Comparing these laws with the experimental results would lead to the determination of the rate-limiting step and to an interpretation of the variations of $\Phi(P_{O_2})$. Besides, the modelling of the sigmoidal shape of the kinetic curves $\alpha(t)$ is under investigation.

References

[1] S. Aronson, R.B. Roof, J. Belle, J. Chem. Phys. 27 (1957) 137.
[2] R.J. Mc Eachern, P. Taylor, J. Nucl. Mater. 254 (1998) 87.
[3] P. Dehaudt, compte-rendu DEC 99002, 1999.
[4] R.J. Mc Eachern, J. Nucl. Mater. 245 (1997) 238.
[5] D.E.Y. Walker, J. Appl. Chem. 15 (1965) 128.
[6] P. Taylor, D.D. Wood, A.M. Duclos, J. Nucl. Mater. 189 (1992) 116.
[7] L.E. Thomas, O.D. Slagle, R.E. Einziger, J. Nucl. Mater. 184 (1991) 117.
[8] L.E. Thomas, R.E. Einziger, R.E. Woodley, J. Nucl. Mater. 166 (1989) 243.
[9] P.E. Blackburn, J. Weissbart, E.A. Gulbransen, J. Phys. Chem. 62 (1958) 902.
[10] J.S. Anderson, L.E.J. Roberts, E.A. Harper, J. Chem. Soc. (1955) 3946.
[11] T. Gilardi, PhD thesis, Université de Provence, 1993.
[12] P.A. Tempest, P.M. Tucker, J.W. Tyler, J. Nucl. Mater. 151 (1988) 251.
[13] P. Taylor, E.A. Burgess, D.G. Owen, J. Nucl. Mater. 88 (1980) 153.
[14] K.K. Bae, B.G. Kim, Y.W. Lee, M.S. Yang, H.S. Park, J. Nucl. Mater. 209 (1994) 274.
[15] M. Avrami, J. Chem. Phys. 8 (1940) 212.
[16] W.A. Johnson, R.F. Mehl, Trans. Am. Inst. Min. (Metall.) Eng. 135 (1939) 416.
[17] R.J. Mc Eachern, J.W. Choi, M. Kolar, W. Long, P. Taylor, D.D. Wood, J. Nucl. Mater. 249 (1997) 58.
[18] K. Surla, F. Valdivieso, M. Pijolat, M. Soustelle, M. Prin, Solid State Ionics 143 (2001) 355.
[19] M. Tupin, M. Pijolat, F. Valdivieso, M. Soustelle, A. Frichet, P. Barberis, J. Nucl. Mater. 117 (2003) 130.
[20] K. Nahdi, S. Perrin, M. Pijolat, F. Rouquerol, N. Ariguib, M. Ayadi, Phys. Chem. Chem. Phys. 4 (2002) 1972.
[21] J.H. Sharp et al., J. Am. Ceram. Soc. 49 (1966) 379.
[22] A.K. Galway, M.E. Brown, Thermal Decomposition of Ionic Solids, Elsevier, 1999.
[23] M. Pijolat, F. Valdivieso, M. Soustelle, Thermochim. Acta 439 (2005) 86.
[24] Coach software, THERMODATA-INPG-CNRS.
[25] J.P. Viricelle, M. Pijolat, M. Soustelle, J. Chem. Soc. Faraday Trans. 91 (24) (1995) 4437.